Tectonophysics 663 (2015) 192–202

Contents lists available at ScienceDirect

Tectonophysics

journal homepage: www.elsevier.com/locate/tecto

From the Bay of Biscay to the High Atlas: Completing the anisotropic characterization of the upper mantle beneath the westernmost Mediterranean region

J. Díaz [a,*], J. Gallart [a], I. Morais [c], G. Silveira [c,d], D. Pedreira [b], J.A. Pulgar [b], N.A. Dias [c,d], M. Ruiz [a], J.M. González-Cortina [b]

[a] ICTJA-CSIC, c/ Sole Sabaris sn, 08080 Barcelona, Spain
[b] Dep. de Geología, Universidad de Oviedo, c/ J. Arias de Velasco, s/n, 33005 Oviedo, Spain
[c] Instituto Dom Luiz-IDL, Campo Grande, Edifício C8, 1749-016 Lisbon, Portugal
[d] Instituto Superior de Engenharia de Lisboa-ISEL, R. Conselheiro Emídio Navarro, 1959-007 Lisbon, Portugal

ARTICLE INFO

Article history:
Received 12 January 2015
Received in revised form 27 February 2015
Accepted 15 March 2015
Available online 25 March 2015

Keywords:
Anisotropy
SKS splitting
Mantle flow
Iberia
Morocco
Western Mediterranean

ABSTRACT

The knowledge of the anisotropic properties beneath the Iberian Peninsula and Northern Morocco has been dramatically improved since late 2007 with the analysis of the data provided by the dense TopoIberia broad-band seismic network, the increasing number of permanent stations operating in Morocco, Portugal and Spain, and the contribution of smaller scale/higher resolution experiments. Results from the two first TopoIberia deployments have evidenced a spectacular rotation of the fast polarization direction (FPD) along the Gibraltar Arc, interpreted as an evidence of mantle flow deflected around the high velocity slab beneath the Alboran Sea, and a rather uniform N100°E FPD beneath the central Iberian Variscan Massif, consistent with global mantle flow models taking into account contributions of surface plate motion, density variations and net lithosphere rotation. The results from the last Iberarray deployment presented here, covering the northern part of the Iberian Peninsula, also show a rather uniform FPD orientation close to N100°E, thus confirming the previous interpretation globally relating the anisotropic parameters to the LPO of mantle minerals generated by mantle flow at asthenospheric depths. However, the degree of anisotropy varies significantly, from delay time values of around 0.5 s beneath NW Iberia to values reaching 2.0 s in its NE corner. The anisotropic parameters retrieved from single events providing high quality data also show significant differences for stations located in the Variscan units of NW Iberia, suggesting that the region includes multiple anisotropic layers or complex anisotropy systems. These results allow to complete the map of the anisotropic properties of the westernmost Mediterranean region, which can now be considered as one of best constrained regions worldwide, with more than 300 sites investigated over an area extending from the Bay of Biscay to the Sahara platform.

1. Introduction

The investigation on the anisotropic properties of the uppermost mantle is one of the best approaches to better understand the geodynamic processes affecting this depth range. The origin of the upper mantle anisotropy has been classically related to the strain-induced lattice preferred orientation (LPO) of the mantle minerals, in particular of olivine (e.g., Nicolas and Christensen, 1987) developed in response to tectonic flow. Even if the relationship between deformation and anisotropy properties is not straightforward, in tectonically active areas (mid-ocean ridges, rifts, subduction zones) fast polarization directions (FPDs) are expected to mark the direction of mantle flow, while in zones without present-day large-scale tectonic activity, FPD can be related to the strain from the last significant tectonic episode preserved in the subcrustal lithosphere, to dynamic flow in the asthenosphere or to the combined effect of both mechanisms (Savage, 1999; Silver, 1996; Vauchez et al., 2012).

Uppermost mantle anisotropy can be explored using different seismic methodologies, including surface wave scattering, Pn tomography, P wave travel-time azimuthal variation and shear-wave splitting, the latter being widely accepted as the most fructiferous approach. When traveling across an anisotropic medium, a shear wave will split in two waves orthogonally polarized and traveling with different velocities, which will arrive to the seismic station separated by a certain time delay. As this delay is smaller than the period of the teleseismic shear-waves, the polarization of these waves is not linear but shows a characteristic ellipticity. SKS waves, which travel as compressional waves through the external core and are converted again to shear waves in the core mantle boundary (CMB) grossly beneath the station

* Corresponding author. Tel.: +34 4095410.
E-mail address: jdiaz@ictja.csic.es (J. Díaz).

http://dx.doi.org/10.1016/j.tecto.2015.03.007
0040-1951/

are widely used to investigate anisotropy, as their waypaths assure that any anisotropic effect detected must be generated near vertically beneath the receiver station, hence providing a good lateral resolution. On the contrary, the method does not provide direct constrains on the vertical position of the anisotropic zone. During the last decades a large amount of contributions have analyzed SKS splitting in many tectonic settings, from the oldest cratons to active subduction zones (e.g., Long, 2013; Vinnik et al., 2012). As SKS waves have typical periods of 5–10 s, they lay in the middle of the microseismic peak, the zone of the seismic spectra with the largest background noise, mostly related to the interaction of oceanic waves. This makes difficult to get clear SKS arrivals, even for large magnitude events. Additionally, SKS waves need to be isolated from other phases traveling with similar apparent velocities, thus limiting the distance range of useful events to 85°–120°. The first contributions in the 1980s and 1990s (Silver and Chan, 1988; Vinnik et al., 1989) were based in the data from the scarce number of permanent broad band stations deployed worldwide. With the availability of an increasing number of portable broad-band seismometers, experiments focused on anisotropy started to be carried out at local scale using dense deployments recording data during weeks to months. Those studies have been typically focused in relatively small areas or devoted to study larger regions by means of high density linear profiles crossing their main structures. The EarthScope project, started in 2005 in the United States, marked the beginning of a new era in seismic exploration, as it involved the deployment of an homogeneous network of broad-band stations covering the contiguous USA with a regular grid of about 70 km × 70 km. Regarding anisotropic studies, the EarthScope project allowed to obtain very detailed results, including, for example, the observation of toroidal flow around the Juan de Fuca plate (Zandt and Humphreys, 2008). The Iberarray seismic network, integrated in the large-scale TopoIberia project (Díaz et al., 2009), has allowed deploying a similar network in Iberia and northern Morocco. Using more than 70 broad-band instruments and three different deployments, and integrating the permanent stations in the area, the experiment provided a final database holding more than 300 sites, forming a 60 km × 60 km grid and covering a region of approximately 600.000 km^2. Therefore, the TopoIberia network is one of the first examples of high density regional scale seismic experiment providing information on large scale regions with unprecedented detail.

The anisotropic analysis of the first TopoIberia deployments, covering North Morocco and the Southern and central part of the Iberian Peninsula, have already been published by Díaz et al. (2010) and Diaz and Gallart (2014). The objective of this contribution is twofold; firstly, we will present the anisotropic results derived from the data recorded during the last TopoIberia deployment, covering the northern part of Iberia, from the Mediterranean Sea to the Atlantic passive margin (Fig. 1). Secondly, the results from the three deployments will be summarized in order to get, for the first time, a comprehensive image of the anisotropic properties of the westernmost Mediterranean region. In order to complete this image, we present also the anisotropic parameters derived from the analysis of broadband seismic stations in Portugal, including permanent sites and the stations deployed in the framework of the WILAS project, an independent experiment designed to complete the Iberia coverage provided by TopoIberia (see Custodio et al., 2014 for details). The retrieval of the anisotropic properties of this large area allows to further constraining the geodynamic interpretation of the region.

2. Tectonic setting of northern Iberia

The northern part of the Iberian Peninsula has been affected by two large compressional episodes, the Variscan and Alpine orogenies, separated by a period of significant extensional deformation in the Mesozoic.

The Variscan orogeny started with the closure of the Rheic Ocean and the collision between Laurentia-Baltica-Avalonia and the continental margin of Gondwana during the Carboniferous, giving rise to the building of the Pangea supercontinent (Matte, 1991). The western part of northern Iberia is represented by the Variscan Iberian Massif, one of the best-exposed sections of the Variscan belt in Europe, formed mainly by granitoids and metasediments of Precambrian/Paleozoic ages that remained tectonically stable (although locally affected by the western termination of the Alpine orogeny) for the last 300 Ma (Gibbons and Moreno, 2002). The geological trends of the Variscan orogen in North-Iberia show an overall E-verging structure, later complicated by the development of the Ibero-Armorican Arc (or Cantabrian Orocline) in the latest Carboniferous (Gutiérrez Alonso et al., 2012). This massif shows a well-established zonation, based on structural, metamorphic and paleogeographic differences (Farias et al., 1987; Julivert et al., 1972). The Cantabrian Zone is the most external unit and represents the thin-skinned foreland fold-and-thrust belt (Pérez-Estaún et al., 1988, 1994). To the west, the transition to the hinterland zones is represented by the West Asturian-Leonese Zone (WALZ), with westward-increasing metamorphism and internal deformation (Martínez Catalán et al., 1990). Finally, the most internal part of the orogen is located in the western end of northern Iberia and is divided into the Central Iberian Zone (CIZ) and the Galicia-Tras-os-

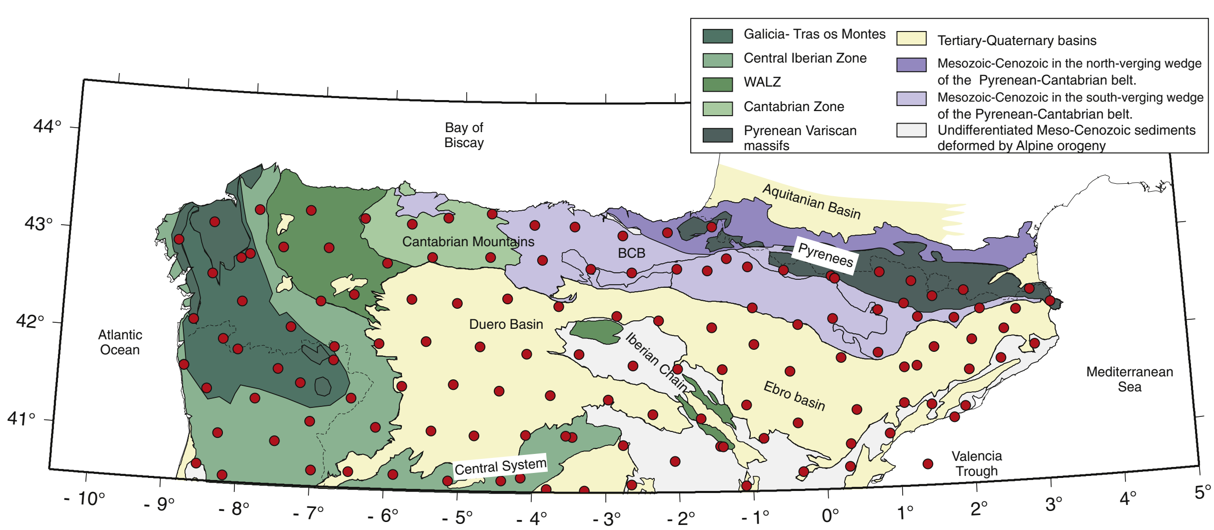

Fig. 1. Simplified geological map of north Iberia showing the locations of the investigated stations, including TopoIberia and WILAS deployments and permanent sites.

Montes Zone (GTMZ), corresponding respectively to autochthonous units and a group of para-autochthonous and allochthonous units including the suture units of the Variscan orogeny (Farias et al., 1987). These areas are characterized by a widespread presence of granitic rocks.

After the end of the Variscan orogeny and the tightening of the Ibero-Armorican Arc in the latest Carboniferous, a period of extensional deformation related to the opening of the Central Atlantic lasted most of the Mesozoic period. The West-Iberian margin and its conjugate, the Newfoundland margin formed during two successive rifting events: one in the Late Triassic to Early Jurassic, and a second and more important one during Late Jurassic to Early Cretaceous, leading to seafloor spreading of the southern North Atlantic (Ranero and Pérez-Gussinyé, 2010; Sutra et al., 2013; Tucholke et al., 2007). Another rift arm developed in the northern border of Iberia, which began to diverge from Eurasia. Very deep basins were created in between, such as the Parentis, Basque-Cantabrian and Mauléon basins. A bit further south, the Iberian Basin developed in an intraplate context. In the western part of North-Iberia, north of the present-day shoreline, extension lead to the opening of the Bay of Biscay between the North-Iberian (or Cantabrian) margin and its conjugate, the Armorican margin. Seafloor spreading occurred in the western part of the bay during mid to Late Cretaceous times (e.g. Sibuet et al., 2004).

Since the latest Cretaceous and during most of the Tertiary, the northward drift of the African Plate forced the convergence between Iberia and Eurasia as the western termination of the Alpine orogeny. This event produced the inversion of the Mesozoic sedimentary basins and the uplift of basement blocks and thrust sheets in the contact zone, shortening the former passive margin and building up the doubly-vergent Pyrenean-Cantabrian mountain belt (e.g. Alonso et al., 1996; Boillot and Malod, 1988; Gallastegui et al., 2002; Muñoz, 1992; Pedreira et al., 2007, 2015). The north-verging wedge of this orogen is prolonged from the Pyrenees to the North-Iberian margin, crossing the NE corner of the Basque-Cantabrian Basin. The south-verging wedge continues through the Cantabrian Mountains, which include the inverted Basque-Cantabrian Basin and parts of the Variscan Iberian Massif to the west, uplifted along a major basement thrust (Alonso et al., 1996). This E–W trending orogen is bounded by the Aquitanian foreland basin to the north and by the Duero and Ebro foreland basins to the south. The deep structure of northern Iberia has been recently imaged using tomographic methods by Chevrot et al. (2014). This new teleseismic tomography seems to rule out the subduction of oceanic lithosphere beneath the Pyrenean Chain, rather supporting the hypothesis that the Pyrenees are the result of the tectonic inversion of a continental rift. The central part of the Iberian Peninsula is marked by the Meseta, an uplifted plateau with a mean altitude of around 700 m, probably the highest in Europe, which still lacks for a fully accepted explanatory model, even if it has been related to a low velocity zone in the upper mantle imaged by tomographic models (Carballo et al., 2015). This Meseta is mainly occupied by the Duero basin to the north and the Tagus basin to the south, separated by the Central Iberian System, an ENE–WSW-oriented intraplate mountain range uplifted as a crustal pop-up developed in the Variscan basement during the Alpine orogeny (e.g. de Vicente et al., 2007 and references therein). To the east, another Alpine-age mountain belt developed by the inversion of the Mesozoic Iberian basin, also involving the Variscan basement: the Iberian Chain (Guimerà et al., 2004). This chain links to the SE with the Catalan Coastal Ranges, another alpine mountain system developed along the Mediterranean coast. Offshore, the Valencia Trough was opened during the Neogene clockwise rotation of the Balearic Islands, and it is considered to represent the southwestern prolongation of the Provençal basin, linked in turn to the counterclockwise rotation of the Corsica-Sardinia block (Dewey et al., 1989). These basins were formed in a back-arc settings on top of the western Mediterranean subducting slab, with a complex evolution complicated by the northeastern prolongation of the Betics compressional deformation along the Balearic Promontory (Faccenna et al., 2014; Fontboté et al., 1990; Negredo et al., 1999).

3. Data acquisition and processing

The third Iberarray deployment started in fall 2010 and was fully operational as of spring 2011. Most of the stations remained active until the end of the project, in summer 2013, hence providing more than two years of available data. Data from the permanent networks have been analyzed for the period 2010–2013, thus gathering about 3 years of teleseismic recordings. This has resulted in a dataset comprising 98 stations to be added to the nearly 200 sites previously investigated by Díaz et al. (2009) and Díaz and Gallart (2014). using data from the first and second TopoIberia deployments. All the earthquakes with magnitude greater than 6.0–6.2 and epicentral distances ranging between 90° and 130° have been inspected and up to 79 events have finally provided useful anisotropic measurements.

To inspect this large amount of data we have benefited from the SplitLab software (Wüstefeld et al., 2008), that provides a useful tool to measure the splitting parameters and manage the resulting database. Consistently with Díaz and Gallart (2014), we have favored the method based on the search for a maximum correlation between the two quasi-shear waves as it is less sensitive to possible mis-orientations of the seismometer horizontal components than the methods based on the minimization of the transverse component energy (Tian et al., 2011).

Standard quality criteria are used, based on i) a good signal-to-noise ratio allowing clear phase identifications and ii) the retrieval of a linear particle motion consistent with the event back azimuth once the anisotropic effect has been corrected. According to these criteria, the measurements were classified into three categories (good, fair, poor) and only those in the first two classes were retained (Fig. 2).

As SKS waves have a dominant period ranging from 5 to 10 s, it is difficult to get accurate measurements of small delay times. As a general rule, only the events with delay times greater than 0.4 s are classified as anisotropic. Events resulting in smaller delay times are classified as showing no evidence of anisotropy and usually referred as “nulls”. Assuming hexagonal symmetry and a horizontal symmetry axis, only those events with back azimuth close to one of the principal axes are expected to result in nulls. Therefore, the identification of signal without evidences of anisotropy along a significant azimuthal range needs to be interpreted carefully. However, if the signal to noise ratio is small, the amplitude of the background seismic noise can mask the arrival of the quasi-shear waves, leading to the observation of a large number of apparent nulls. To avoid classifying noisy events with unstable measurements as nulls, we have only retained those measurements providing delay times smaller than 0.25 s and discarded those with delay times between 0.25 s and 0.4 s. This resulted in a total of 870 non-null and 318 null measurements. For most of the stations we have retained 8 to 20 observations, with a mean value of 13 valid measurements per station.

The anisotropy beneath Portugal has been analyzed using data from permanent broad-band stations and from the WILAS experiment, involving the deployment of a dense array of temporary stations (Custodio et al., 2014). The portable stations were active during a period of nearly 2 years, from July 2010 to June 2012, to overlap with the 2nd and 3rd TopoIberia deployments. WILAS also provided the necessary framework for data-sharing between all other broad-band seismic networks operating in Portugal. For the permanent stations, a larger

Fig. 2. Example of the splitting parameters obtained using the SplitLab software. a) Example of a good quality non-null measurement at station E114, located in the Iberian Chain, showing a FPD oriented N114°E and $\delta t = 0.9$ s. b) Example of a good quality event at station CCAS, located close to the northern Mediterranean shoreline, showing a much larger $\delta t = 1.8$ s and a similar N100°E oriented FPD. c) Example of “null” measurement at station E153, located in the Cantabrian zone, for an event with N25°E back azimuth.

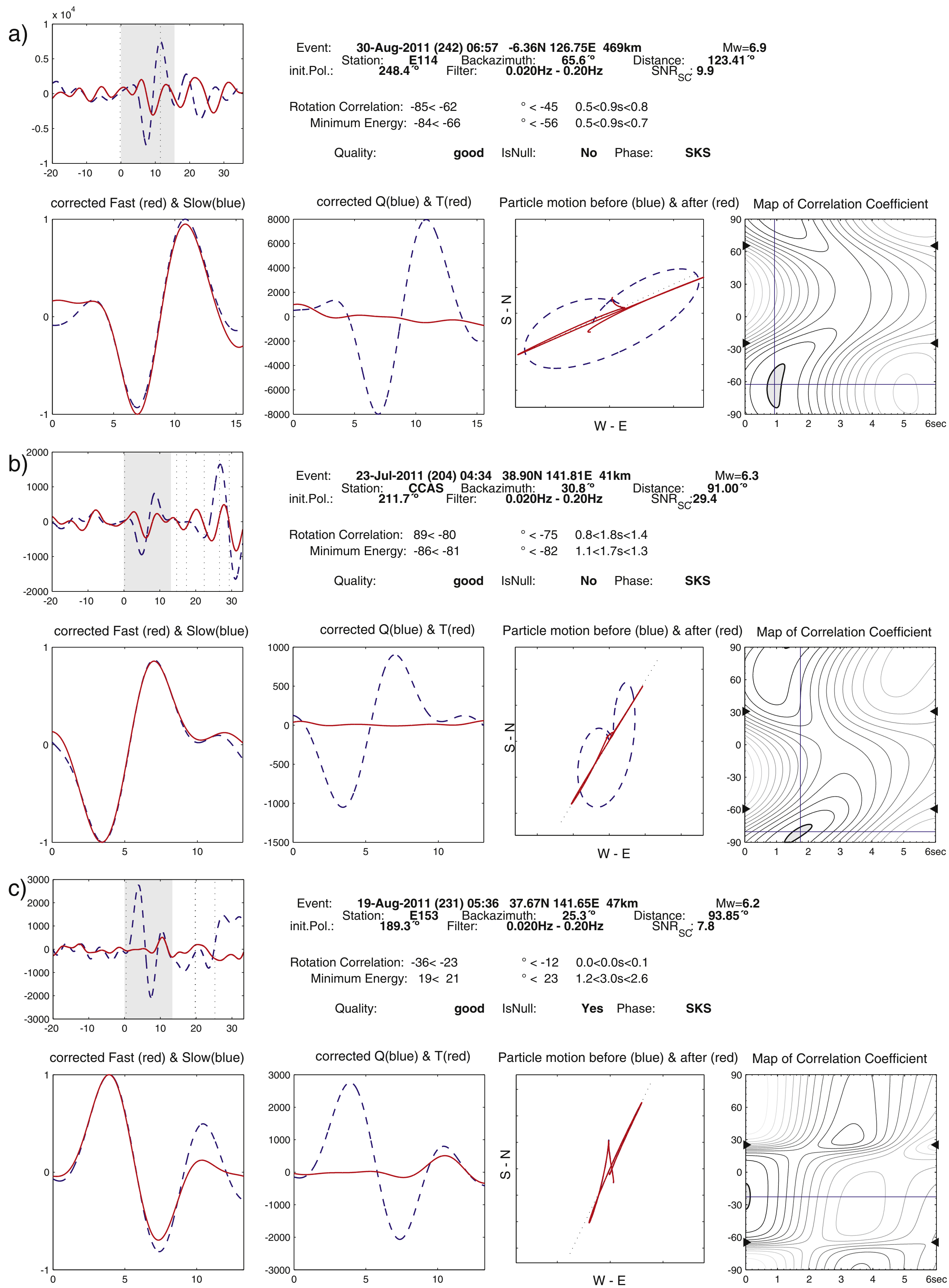
a)
Event: 30-Aug-2011 (242) 06:57 -6.36N 126.75E 469km Mw=6.9
Station: E114 Backazimuth: 65.6° Distance: 123.41°
init.Pol.: 248.4° Filter: 0.020Hz - 0.20Hz SNRSC: 9.9
Rotation Correlation: -85< -62 ° < -45 0.5<0.9s<0.8
Minimum Energy: -84< -66 ° < -56 0.5<0.9s<0.7
Quality: good IsNull: No Phase: SKS
corrected Fast (red) & Slow(blue)
corrected Q(blue) & T(red)
Particle motion before (blue) & after (red)
Map of Correlation Coefficient
S - N
W - E
b)
Event: 23-Jul-2011 (204) 04:34 38.90N 141.81E 41km Mw=6.3
Station: CCAS Backazimuth: 30.8° Distance: 91.00°
init.Pol.: 211.7° Filter: 0.020Hz - 0.20Hz SNRSC:29.4
Rotation Correlation: 89< -80 ° < -75 0.8<1.8s<1.4
Minimum Energy: -86< -81 ° < -82 1.1<1.7s<1.3
Quality: good IsNull: No Phase: SKS
corrected Fast (red) & Slow(blue)
corrected Q(blue) & T(red)
Particle motion before (blue) & after (red)
Map of Correlation Coefficient
S - N
W - E
c)
Event: 19-Aug-2011 (231) 05:36 37.67N 141.65E 47km Mw=6.2
Station: E153 Backazimuth: 25.3° Distance: 93.85°
init.Pol.: 189.3° Filter: 0.020Hz - 0.20Hz SNRSC: 7.8
Rotation Correlation: -36< -23 ° < -12 0.0<0.0s<0.1
Minimum Energy: 19< 21 ° < 23 1.2<3.0s<2.6
Quality: good IsNull: Yes Phase: SKS
corrected Fast (red) & Slow(blue)
corrected Q(blue) & T(red)
Particle motion before (blue) & after (red)
Map of Correlation Coefficient
S - N
W - E
6sec

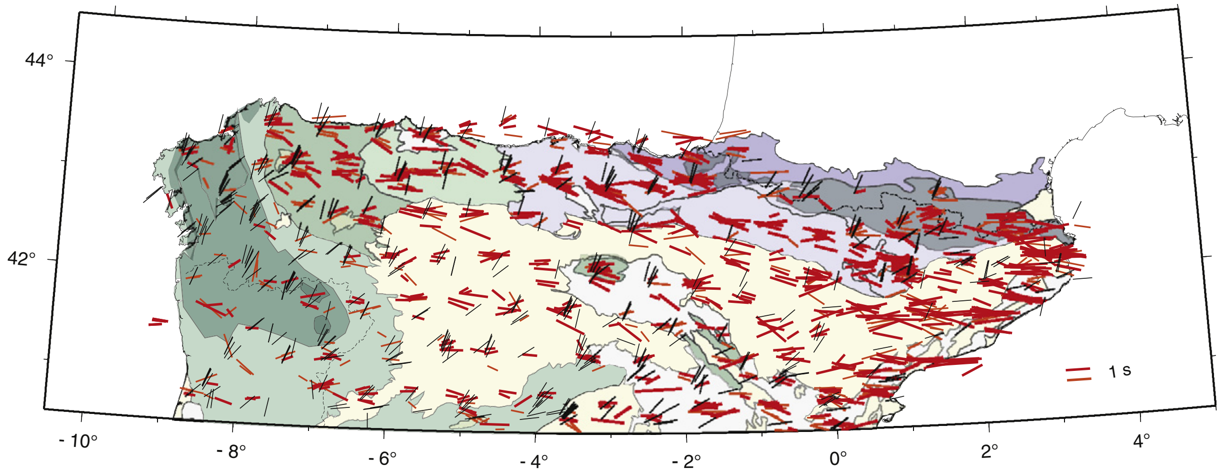

Fig. 3. Anisotropic parameters retrieved from our dataset overprinting a simplified tectonic map of the region. The results are presented in the projected location of the piercing point at a depth of 200 km. Bars are oriented along the FPD and their length is proportional to the measured δt. Thin black lines represent event without splitting evidence (nulls) and are oriented following the back azimuthal direction.

time period, extending from 2008 to 2012 has been analyzed. In the particular case of the MTE station, located in central-north Portugal, in the western part of the Iberian Massif, we have benefited from the previous contribution by Morais (2012), who inspected the 1997–2004 period. The analysis of the Portuguese stations was performed using the approach of Vinnik et al. (1989). In this method the SKS waveforms, chosen to maximize azimuthal coverage, are first stacked to minimize noise effects as well as the bias introduced by the strongest events. The transverse component of SKS and similar phases is synthesized from the observed radial component for a number of different anisotropic models. The optimum model is obtained by minimizing the difference between the synthetic and observed transverse component, using a penalty function.

Data from some of the Portuguese stations has also been investigated using the SplitLab program to validate the consistency of the results obtained by both approaches, giving typical differences in FPD of around 10°/15° and hence allowing the integration of the results.

Even if SKS measurements do not provide direct constrains on the vertical position of the anisotropic zone, it is widely accepted that most of the anisotropy comes from the upper mantle, even if it remains unclear whether anisotropy is confined to the uppermost mantle or continues through the transition zone (Savage, 1999). Therefore we have chosen to present the individual results in Fig. 3 located on the vertical of their piercing points at a representative depth fixed of 200 km. Supplementary Table 1 provides a complete list of each measurement and Supplementary Table 2 shows the geographical coordinates and the mean FPD and delay time (δt) for each analyzed station.

The inferred FPD values are quite uniform across northern Iberia, with mean orientations close to N100°E, and are generally consistent with the scarce data previously available, arising from short-term deployments in the Pyrenees (Barruol et al., 1998), the Cantabrian Mountains and Galicia (Díaz et al., 2006). Stations in the Pyrenean Range and NE Iberia show a slightly different FPD, closer to a WNW–ESE direction, even if it is difficult to assess the validity of this variation. On the contrary, the δt values show a clear E–W change, with values below 0.6 s in the western part of Iberia, mean values of around 1.0 s in the central part, the Pyrenees and the Ebro basin and reaching values close to 2.0 s near the coast of the Mediterranean Sea. The number of null measurements is also inhomogeneous, with an increased number in the western sites and also for stations close to the Central System. It is important to note that most of the retained nulls have common back azimuthal directions.

Most of the investigated stations show azimuthal dependence on its anisotropic properties. Fig. 4a illustrates this dependence for some representative stations. It can be observed that FPDs are close to EW for events with NE back azimuth and shift clockwise with the back azimuth. In the third quadrant, we found an equivalent variation, with FPD close to EW for SW back azimuths and shifting to N130°E as back azimuth approaches to W. This figure also shows the change in δt along an EW transect. However we must point out that the azimuthally dependent FPD variation remains moderate, as it spans on a 30–40° range. Such kind of dependence is typically explained by the presence of multiple anisotropic layers at different depth ranges (e.g. Silver and Savage, 1994). Since the usual earthquake distribution around the planet does not allow to cover the second and forth quadrants with a satisfactory number of events, it becomes very difficult to get a good back azimuthal coverage allowing to infer a realistic model to explain those second order variations.

Fig. 4b documents the differential anisotropic parameters observed in the western part of northern Iberia, by presenting the anisotropic parameters retrieved for 2 events with back azimuths close to SW and E directions. The first case shows rather uniform results, with FPD close to EW for most of the stations in northern Iberia, except those located in western area and some of those along the Duero basin and the Iberian Chain, where “nulls” are consistently detected. The event with E back azimuth provides clearly different results. Most of the stations give now null measurements, consistently with an anisotropic model with an EW oriented FPD. On the other hand, stations located in the NW corner of the Iberian Peninsula consistently show for the same event a non-null, N130°E oriented FPD.

These results allow to complete the high resolution exploration of anisotropy beneath Iberia resulting from the analysis of the TopoIberia project Díaz et al., 2009, Diaz and Gallart, 2014). Fig. 5 summarizes this information by presenting a complete map of the anisotropic parameters in the westernmost Mediterranean region, extending from the Sahara platform to the Bay of Biscay and covering the whole Iberian Peninsula. Prior results included in the SKS splitting data base (Wüstefeld et al., 2009, http://splitting.gm.univ-montp2.fr) are also included in the map. In order to get a more accurate view of the variations in the anisotropic parameters across the investigated region, we have located each individual measurement in the vertical of its piercing point at a depth of 200 km and built a continuous map using the nearest neighbor gridding algorithm included in the GMT package (Wessel and Smith, 1998). The resulting maps are presented in Fig. 6 and will be discussed in the next section.

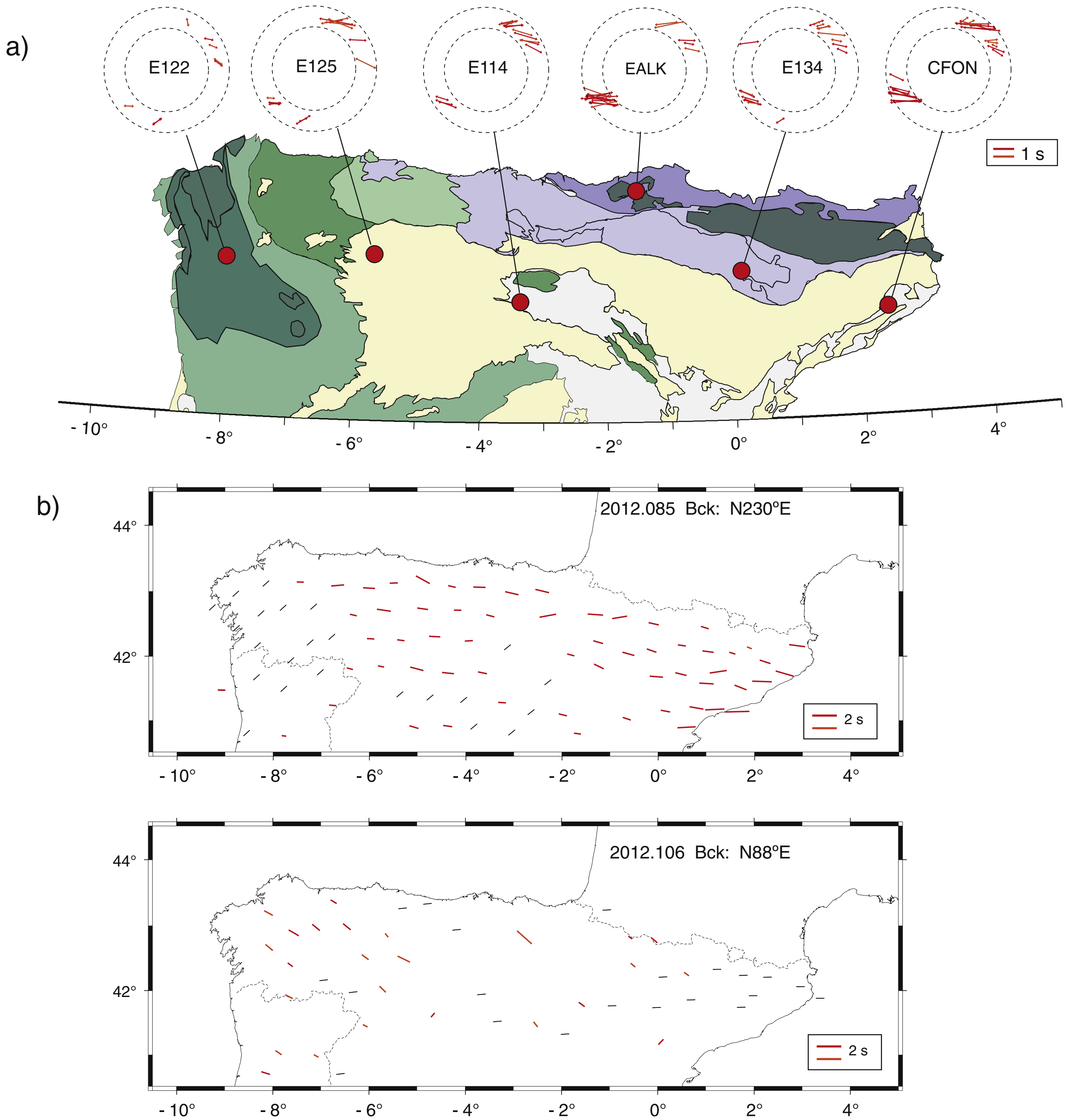

Fig. 4. a) Individual anisotropic measurements for a selected group of representative stations along an E–W profile. For each station, the bars representing FPD are displayed around a circle following its back azimuthal direction. b) Anisotropic parameters for 2 selected events reaching northern Iberia along different back azimuthal directions at all the stations providing useful results. Bars are oriented along the FPD and their length is proportional to the measured δt. Red bars are for "good" quality measurements while orange bars stand for "fair" results. "Null" measurements are represented by thin black lines oriented along the back azimuth.

4. Geodynamic interpretation

In order to interpret geodynamically the anisotropic parameters, a good knowledge of the mechanism responsible for the anisotropy is needed. It has been established that the crust contribution to the delay times observed between split SKS waves is limited to few tens of second and hence that most of the anisotropy comes from the upper mantle, even if it remains unclear whether anisotropy is confined to the upper 200 km or it continues through the transition zone (Savage, 1999; Yuan and Beghein, 2013). It is also widely accepted that anisotropy in the mantle is mostly related to the lattice preferred orientation (LPO) of the minerals, in particular olivine, which is the major constituent of the upper mantle (Nicolas and Christensen, 1987). Laboratory experiments have shown that the fast propagation axes in peridotites aligns with the direction of maximum shear, although factors such as temperature, melt fraction or presence of water result in changes in the olivine fabric and its relationship with deformation (Long and Becker, 2010). For most kinds of finite strain, FPDs are thus expected to be parallel to the extension direction (Silver and Chan, 1988). In tectonically active areas the present-day mantle flow can explain the peridotite LPO. Vinnik et al. (1992) proposed that the passive motion of the lithosphere over the asthenospheric mantle will result in FPD oriented parallel to the absolute plate motion. Recent global flow models have shown that the effect of lateral heterogeneity in viscosity, which induce net

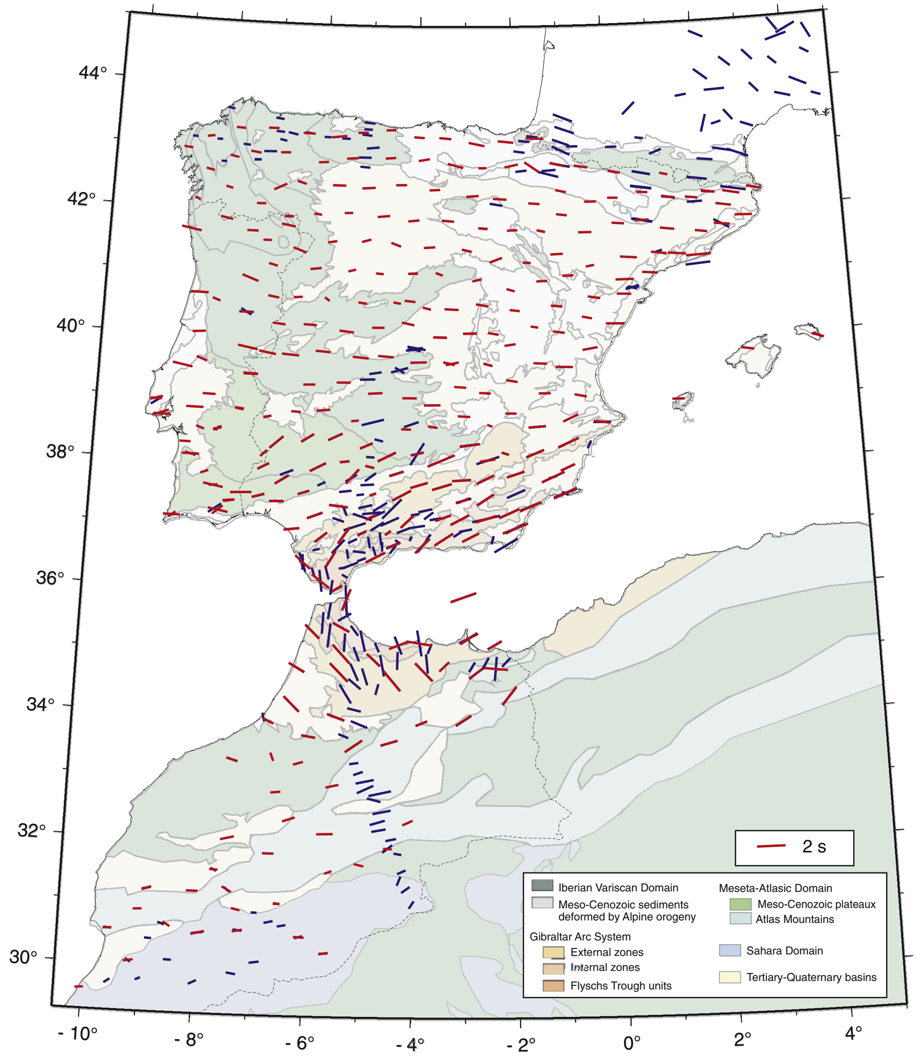

Fig. 5. Final anisotropic map of the Iberian Peninsula and northern Morocco resulting from the analysis of the TopoIberia and complementary recent experiments. Red bars represent the mean FPD obtained for each investigated station. Blue bars are for the previous results in the area, as included in the Montpellier database (Wüstefeld et al., 2009), including the PICASSO results presented by Miller et al. (2013).

lithosphere rotation, and the presence of density-driven flow need also to be taken into consideration (Becker, 2008; Conrad and Behn, 2010; Kreemer, 2009). Under those hypotheses FPD would not be directly related to the absolute plate motion (APM), but will be oriented along the mantle flow direction resulting from the interaction of those processes. If the anisotropy is located in the subcrustal lithosphere, its origin can be related to the last tectonic event affecting the region, which would result in FPD subparallel to major structures, such as plate boundaries or mountains belts. This kind of mechanism has often been invoked to explain anisotropic observations in tectonically passive areas.

The general E–W orientation of the FPD in northern Iberia, indistinctly observed in areas of the Iberian Variscan massif almost undeformed since ~300 Ma and in areas in the north and east overprinted by the Alpine orogeny (Pyrenean–Cantabrian belt), suggest that the general anisotropic pattern is not related to lithospheric “frozen-in” anisotropy acquired in any of these two orogenic events. The clear difference between the FPD retrieved beneath the Central Iberian Massif, close to N100°E, and the surface expression of the arcuate Variscan belt, with tectonic lineaments oriented close to NW–SE in the southern part of Iberia and shifting smoothly to N–S in NW Iberia (Matte, 1991) provides further evidences against a main lithospheric origin of the observed anisotropy (Diaz and Gallart, 2014). If the anisotropic pattern is due to present-day mantle flow, the FPD is expected to be parallel to the mantle flow direction. The first candidate to define the direction of the dominant mantle flow is the APM vector, derived from geodetic models. The APM direction in Iberia depends on the global plate models used; those assuming no net rotation, determined solely from the relative motions between plates, give an absolute plate motion vector oriented close to NE (N50°E) beneath Iberia. This result has been recently confirmed by the results from continuous GPS monitoring obtained in the mainframe of the TopoIberia project (Garate et al., 2014). Models obtained within a hot spot based reference frame, and thus assuming net rotation of the tectonic plates, result in a nearly opposite direction, close to WSW (N238°E) (http://www.unavco.org/community_science/science-support/crustal_motion/dxdt/model.html). Neither of those directions can explain the observed FPD (Fig. 7). The viscous mantle flow model presented by Conrad and Behn (2010), taking into consideration the contributions to global flow of plate tectonics, mantle density heterogeneity and net lithosphere rotation, results in a flow field at upper mantle depths (200–400 km) oriented E–W beneath central Iberia, which is compatible with our splitting measurements. It is important to note that the FPD observed beneath northern Iberia may provide further constrains into the mantle dynamics models for the Mediterranean region. The Fig. 12 in Faccenna et al. (2014) shows that the modification of the upper mantle structure to

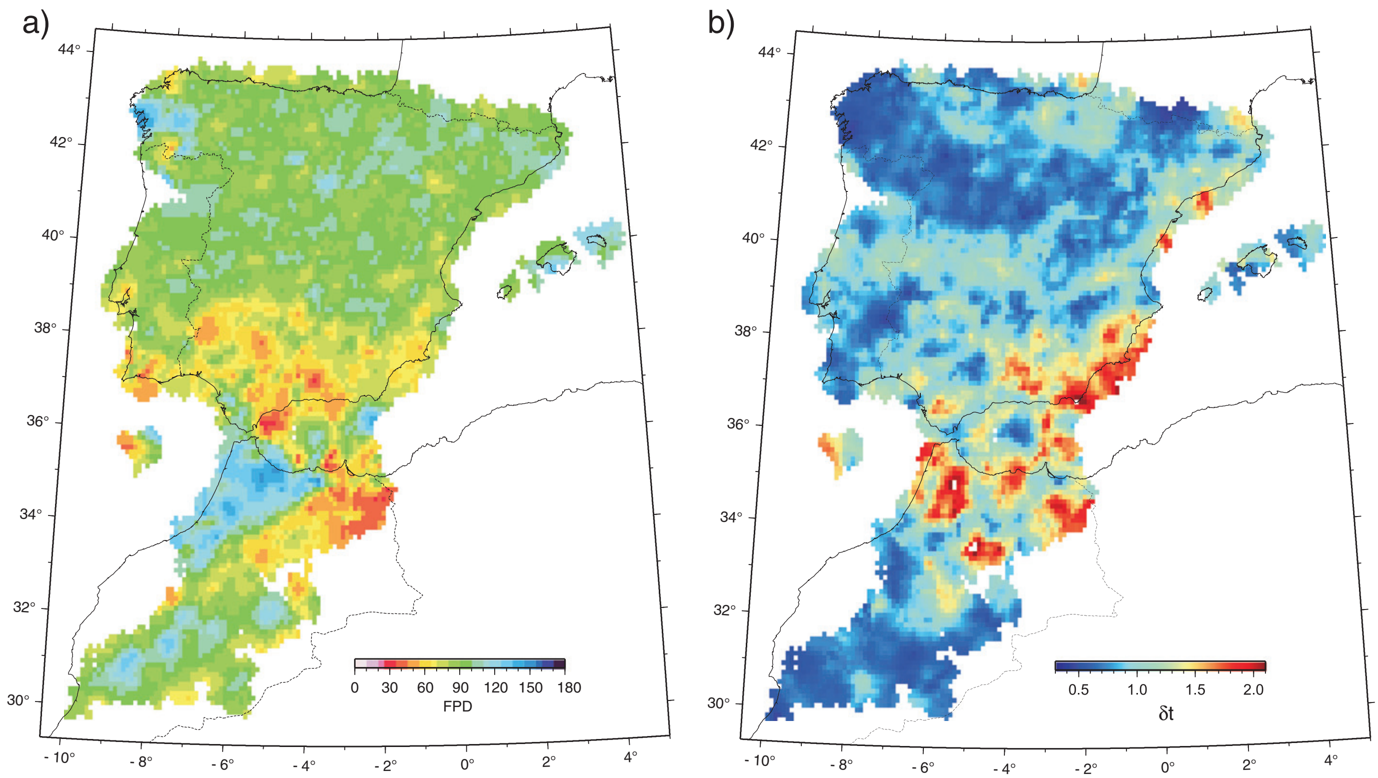

Fig. 6. Gridded maps of the fast polarization directions (a) and the delay times (b) beneath the investigated area. Each measurement is located in the vertical of its piercing point at 200 km and the grid is interpolated using a standard nearest neighbor algorithm.

take into account the Tyrrhenian and Hellenic slabs regions improve the agreement between FPD observations and predictions beneath those regions, but results in a clearly worse adjustment beneath central and northern Iberia, suggesting than further improvements are still needed.

Within this broad picture, the imprint of Variscan and Alpine orogenies can, however, modulate the anisotropic pattern and potentially explain some small-scale anomalies. The FPD retrieved for stations located in the Iberian Massif are clearly different from the crustal expression of the Variscan orogeny, with structures oriented close to NW–SE in the southern part of Iberia and shifting smoothly to N–S in NW Iberia following the arcuate Variscan belt (Matte, 1991). However, there is a striking coincidence between the locus of Variscan synkinematic, I-type granitoids in NW Iberia, and a zone characterized by a slightly more WNW–ESE orientation of FPD, with small δt and a large number of nulls. This introduces the possibility that some "frozen-in" anisotropy in the innermost part of the Variscan orogen contribute to the disorganization of the general asthenospheric E–W anisotropy. This will result in a two-layered anisotropic model involving lithospheric and asthenospheric contributions, at least beneath this zone, even if the characterization of such a model is beyond the objectives of this contribution.

Beneath the Pyrenees and the Cantabrian Mountains, a roughly E–W orogenic belt, the imprint of the Alpine deformation may also contribute partially to the E–W oriented FPD (Barruol et al., 1998; Díaz et al., 2002). However, this contribution must be small, because no significant differences are observed between the anisotropic parameters obtained at stations located in the core of the Pyrenean–Cantabrian mountain belt and those located in its foreland basins. In the central part of Iberia, the Meso-Tertiary zones reworked by the Alpine orogeny, their tertiary foreland basins and the undisturbed Variscan Iberian Massif show also similar anisotropic parameters, suggesting a common mechanism of the observed anisotropy related to present-day asthenospheric flow.

The FPD results presented by Barruol et al. (2004) for eastern Alps and southern France show a smooth pattern with a major NW–SE component. These results were interpreted as resulting from a regional asthenospheric flow induced by the sinking of Apenninic slab and the subsequent rotation of the Corsica-Sardinia block. The northeast area of the Iberian Peninsula shows higher than average δt values, suggesting that the anisotropy beneath this area is still influenced by the regional flow proposed by Barruol et al. (2004).

Moving south, we retrieve the interpretation presented by Diaz and Gallart (2014). The reader is addressed to this contribution for a detailed discussion, but we include here a short summary of their main points for completeness. The arcuate variation in the FPD along the Gibraltar Arc, already pointed by Buontempo et al. (2008) using a limited set of data, is explained by the deflection of the global mantle flow around the fast velocity slab depicted by tomography beneath the Alboran Sea (Bezada et al., 2013; Bonnin et al., 2014). This deflection will also explain the progressive FPD shift observed in southern Iberia, from NE–SW in the West to ENE–WSW in the eastern part, as well as the abrupt change in FPD in the northern coast of Morocco at about 3°W (Alhoceima region). As the global mantle flow of Conrad and Behn (2010) does not take into consideration the presence of the Alboran slab, a large discrepancy between the model and the actual FPD is observed beneath this region (Fig. 7). It is worthy to note that evidences of similar mantle flow have been documented beneath other areas of the Mediterranean region, particularly beneath the Calabrian Arc (Baccheschi et al., 2011) or the Aegean (Evangelidis et al., 2011). Different authors (Faccenna et al., 2014; Jolivet et al., 2009) have indeed proposed that the presence of asthenospheric flow around small-scale subducted slabs is a characteristic feature of Mediterranean basins. The large number of nulls extending over a large back azimuthal range in SW Portugal and eastern Morocco suggest the presence of mantle flow with a predominant vertical component. This is consistent with models based in potential fields showing large variations in the lithospheric thickness beneath those areas (Fullea et al., 2010; Jiménez-Munt et al., 2011), with S-wave velocity models obtained from joint inversion of Ps and Sp receiver functions (Morais et al., 2015), and with the small-scale, edge-driven convective cells, proposed by Missenard and Cadoux (2011) to account for Cenozoic volcanic activity in the Atlas.

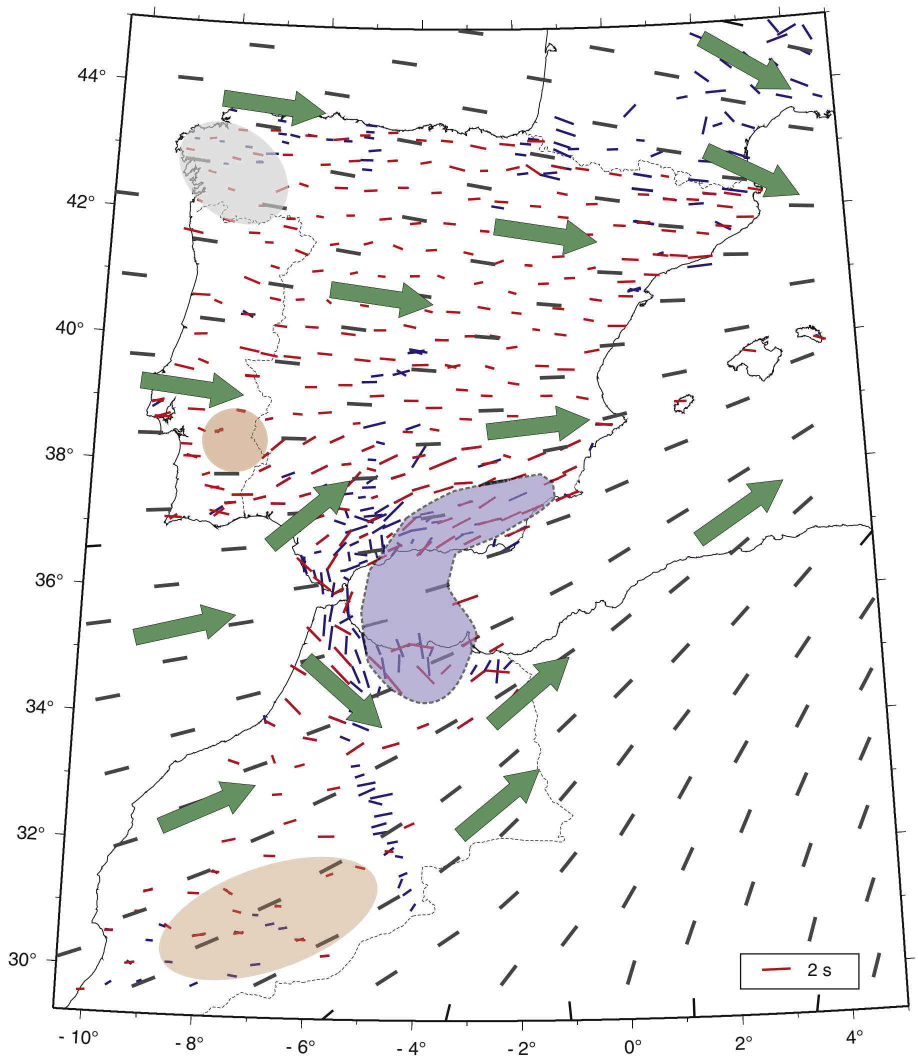

Fig. 7. Sketch illustrating the processes invoked to explain the observed anisotropic parameters. Red and blue lines as in the previous figure. Black lines are for the LPO direction derived from the Conrad and Behn (2010) global mantle flow model. Green arrows show the proposed mantle flow. The blue shadowed area accounts for the high velocity slab anomaly imaged by seismic tomography beneath SW Iberia (Bezada et al., 2013). Brown shadowed areas in SW Portugal and the High Atlas represent the zones where we interpret vertical mantle flow associated to small-scale convective cells. Gray shaded area in NW Iberia is for the zone where a significant amount of lithospheric anisotropy related to the Variscan orogeny is proposed.

5. Conclusions

The last TopoIberia deployment covers the northern part of the Iberian Peninsula, from the eastern Pyrenees to the most hinterland parts of the Variscan belt. The results show an average fast velocity direction close to E–W. The origin of this anisotropy is globally related to the LPO of mantle minerals generated by mantle flow at asthenospheric depths. Delay times of around 1.0 s–1.5 s are observed in most of the stations, but lower values, not exceeding 0.8 s, are measured in the Galicia-Trás-os-Montes zone. We interpret that this zone, corresponding to the core of the Variscan deformation, may have a secondary lithospheric anisotropic layer overprinting the general asthenospheric flow. Sites located near the Mediterranean coast exhibit a clearly higher delay time, close to 2.0 s. This can be related to a regional asthenospheric flow beneath the Ligurian induced by the sinking of the Apenninic slab. The presence of an azimuthal dependence of the splitting parameters is also confirmed by the new data, denoting a complex distribution at depth of the anisotropic features. However, the limited back azimuthal coverage does not allow to investigate the properties of two-layered anisotropic models which could explain satisfactorily the observed patterns. Even if data from short term experiments in the Pyrenees and northern Iberia have previously given a first insight on the anisotropic properties of this region, the analysis of the new dataset provides a much better coverage and resolution, emphasizing the regional variations of the anisotropic properties, as the clearly distinct FPD beneath NW Iberia or the relevant variations in delay time across northern Iberia (Fig. 6b).

From a more general point of view, the results presented here allow to complete the map of the anisotropical features of the westernmost Mediterranean region, which can now be considered as one of the world regions with better anisotropic constraints, with more than 300 sites investigated over an area exceeding 600.000 km^2. The new results tend to confirm the previous interpretation presented by Diaz and Gallart (2014), globally relating the anisotropic parameters to the LPO of mantle minerals generated by mantle flow at asthenospheric depths. The E–W oriented FPD are compatible with mantle flow models taking into consideration the combined effect of relative plate motions, mantle density heterogeneity and net lithosphere rotation (e.g., Conrad and Behn, 2010). However, the new results confirm also that the anisotropic properties show significant regional variations, which can be related to major geodynamical processes. Hence, the arcuate variation of the FPDs following the Gibraltar Arc is interpreted to result from the mantle flow deflection around the fast velocity slab extending down to 600 km. The small degree of anisotropy and the large number of observations without evidences of anisotropy beneath SW Iberia, the High Atlas and the northern rim of the West African Craton have been interpreted as suggesting the presence of vertical mantle flow associated to edge-driven convective cells triggered by large variations of the lithospheric thickness.

Supplementary data to this article can be found online at http://dx.doi.org/10.1016/j.tecto.2015.03.007.

Acknowledgments

We want to acknowledge all the field and processing Spanish and Moroccan teams of the TopoIberia-Iberarray experiment that made this large dataset available. We want also to acknowledge the institutions responsible for the maintenance of the different permanent seismic networks contributing data to this study (Instituto Geográfico Nacional, Real Observatorio de la Armada, Instituto Andaluz de Geofísica, and Portuguese Seismic Network). This is a contribution of the Consolider-Ingenio 2010 project TOPO-IBERIA [CSD2006-00041]. Additional funding is provided by projects RIFSIS [CGL2009-09727], Siberia [CGL2006-01171] and Topomed [CGL2008-03474-E/BTE, ESF-Eurocores 07-TOPOEUROPE-FP006]. The Portuguese research team was supported by the Fundação para a Ciência e Tecnologia through projects WILAS (PTDC/CTE-GIX/097946/2008) and AQUAREL (PTDC/CTE-GIX/116819/2010). This is a contribution to ID/GEO/50019/2013. Most of the figures were produced using the Generic Mapping Tools (GMT) software (Wessel and Smith, 1998).

References

Alonso, J.L., Pulgar, J.A., García-Ramos, J.C., Barba, P., 1996. Tertiary basins and Alpine tectonics in the Cantabrian Mountains (NW Spain). In: Friend, P.F., Dabrio, C.J. (Eds.), Tertiary Basins of Spain: The Stratigraphic Record of Crustal Kinematics. Cambridge University Press, Cambridge, United Kingdom, pp. 214–227.

Baccheschi, P., Margheriti, L., Steckler, M.S., Boschi, E., 2011. Anisotropy patterns in the subducting lithosphere and in the mantle wedge: A case study—The southern Italy subduction system. J. Geophys. Res. 116, B08306. http://dx.doi.org/10.1029/2010JB007961.

Barruol, G., Souriau, A., Vauchez, A., Díaz, J., Gallart, J., Tubia, J., Cuevas, J., 1998. Lithospheric anisotropy beneath the Pyrenees from shear wave splitting. J. Geophys. Res. 103, 30039–30054.

Barruol, G., Deschamps, A., Coutant, O., 2004. Mapping upper mantle anisotropy beneath SE France by SKS splitting indicates Neogene asthenospheric flow induced by Apenninic slab roll-back and deflected by the deep Alpine roots. Tectonophysics 394, 125–138.

Becker, T.W., 2008. Azimuthal seismic anisotropy constrains net rotation of the lithosphere. Geophys. Res. Lett. 35, L05303. http://dx.doi.org/10.1029/2007GL032928.

Bezada, M.J., Humphreys, E.D., Toomey, D.R., Harnafi, M., Dávila, J.M., Gallart, J., 2013. Evidence for slab rollback in the westernmost Mediterranean from improved upper mantle imaging. Earth Planet. Sci. Lett. 368, 51–60. http://dx.doi.org/10.1016/j.epsl.2013.02.024.

Boillot, G., Malod, J., 1988. The North and North-West Spanish continental margin: a review. Rev. Soc. Geol. Esp. 1 (3–4), 295–316.

Bonnin, M., Nolet, G., Villaseñor, A., Gallart, J., Thomas, Ch., 2014. Multiple-frequency tomography of the upper mantle beneath the African/Iberian collision zone. Geophys. J. Int. 198, 1458–1473. http://dx.doi.org/10.1093/gji/ggu214.

Buontempo, L., Bokelmann, G.H.R., Barruol, G., Morales, J., 2008. Seismic anisotropy beneath Southern Iberia from SKS splitting. Earth Planet. Sci. Lett. 273 (3–4), 237–250. http://dx.doi.org/10.1016/j.epsl.2008.06.024.

Carballo, A., Fernandez, M., Jiménez-Munt, I., Torne, M., Vergés, J., Melchiorre, M., Pedreira, D., Afonso, J.C., García-Castellanos, D., Díaz, J., Villaseñor, A., Pulgar, J., Quintana, L., 2015. From the North Iberian Margin to the Alboran Basin: a lithosphere geo-transect crossing the Iberian Plate. Tectonophys 663, 399–418.

Chevrot, S., Villaseñor, A., Sylvander, M., Benahmed, S., Beucler, E., Cougoulat, G., Delmas, P., de Saint Blanquat, M., Diaz, J., Gallart, J., Grimaud, F., Lagabrielle, Y., Manatschal, G., Mocquet, A., Pauchet, H., Paul, A., Péquegnat, C., Quillard, O., Roussel, S., Ruiz, M., Wolyniec, D., 2014. High-resolution imaging of the Pyrenees and Massif Central from the data of the PYROPE and IBERARRAY portable array deployments. J. Geophys. Res. 119 (8), 6399–6420. http://dx.doi.org/10.1002/2014JB010953.

Conrad, C.P., Behn, M.D., 2010. Constraints on lithosphere net rotation and asthenospheric viscosity from global mantle flow models and seismic anisotropy. Geochem. Geophys. Geosyst. 11, Q05W05. http://dx.doi.org/10.1029/2009GC002970.

Custodio, S., Dias, N.A., Caldeira, B., Carrilho, F., Corela, C., Diaz, J., Narciso, J., Madureira, G., Matias, L., Haberland, C., WILAS team, 2014. Ambient noise recorded by a dense broadband seismic deployment in Western Iberia. Bull. Seismol. Soc. Am. http://dx.doi.org/10.1785/0120140079.

De Vicente, G., Vegas, R., Muñoz Martín, A., Silva, P.G., Andriessen, P., Cloetingh, S., González Casado, J.M., Van Wees, J.D., Álvarez, J., Carbó, A., 2007. Cenozoic thick-skinned deformation and topography evolution of the Spanish Central System. Glob. Planet. Chang. 58 (1–4), 335–381.

Dewey, J.F., Helman, M.L., Turco, E., Hutton, D.H.W., Knott, S.D., 1989. Kinematics of the Western Mediterranean. In: Coward, M.P., Dietrich, D., Park, R.G. (Eds.), Alpine Tectonics. Geol. Soc. Spec. Publ. 45. Geological Society of London, London, pp. 265–283.

Diaz, J., Gallart, J., 2014. Seismic anisotropy from the Variscan Core of Iberia to the Western African Craton: new constrains on upper mantle flow at regional scales. Earth Planet. Sci. Lett. 394, 48–57. http://dx.doi.org/10.1016/j.epsl.2014.03.005.

Díaz, J., Gallart, J., Ruiz, M., Pulgar, J.A., López, C., González-Cortina, J.M., 2002. Anisotropic features of the Alpine lithosphere in Northern Spain. Geophys. Res. Lett. 29, 24. http://dx.doi.org/10.1029/2002GL015997.

Díaz, J., Gallart, J., Ruiz, M., Pulgar, J.A., Lopez, C., González-Cortina, J.M., 2006. Probing seismic anisotropy in North Iberia from shear wave splitting. Phys. Earth Planet. Inter. 158, 210–225.

Díaz, J., Villaseñor, A., Gallart, J., Morales, J., Pazos, A., Córdoba, D., Pulgar, J., García-Lobón, J.L., Harnafi, M., TopoIberia Seismic Working, 2009. The IBERARRAY broadband seismic network: a new tool to investigate the deep structure beneath Iberia. Orfeus Newsl. 8, 2.

Díaz, J., Gallart, J., Villaseñor, A., Mancilla, F., Pazos, A., Córdoba, D., Pulgar, J.A., Ibarra, P., Harnafi, M., 2010. Mantle dynamics beneath the Gibraltar Arc (western Mediterranean) from shear-wave splitting measurements on a dense seismic array. Geophys. Res. Lett. 37 (L18304). http://dx.doi.org/10.1029/2010GL044201.

Evangelidis, C.P., Liang, W.T., Melis, N.S., Konstantinou, K.I., 2011. Shear wave anisotropy beneath the Aegean inferred from SKS splitting observations. J. Geophys. Res. 116. http://dx.doi.org/10.1029/2010jb007884.

Faccenna, C., Becker, T.W., Auer, L., Billi, A., Boschi, L., Brun, J.P., Capitanio, F.A., Funiciello, F., Horváth, F., Jolivet, L., Piromallo, C., Royden, L., Rossetti, F., Serpelloni, E., 2014. Mantle dynamics in the Mediterranean. Rev. Geophys. 52, 283–332. http://dx.doi.org/10.1002/(ISSN)1944-9208.

Farias, P., Gallastegui, G., González-Lodeiro, F., Marquínez, J., Martín-Parra, L.M., Martínez-Catalán, J.R., Pablo Maciá, J.G., Rodríguez Fernández, R., 1987. Aportaciones al conocimiento de la litoestratigrafía y estructura de Galicia Central. Mem. Fac. Cienc. Porto 1, 411–431.

Fontboté, J.M., Guimerà, J., Roca, E., Sabat, F., Santanach, P., Fernández-Ortigosa, F., 1990. The Cenozoic geodynamic evolution of the Valencia trough (western Mediterranean). Rev. Soc. Geol. Esp. 3, 7–18.

Fullea, J., Fernández, M., Afonso, J.C., Vergés, J., Zeyen, H., 2010. The structure and evolution of the lithosphere–asthenosphere boundary beneath the Atlantic–Mediterranean transition region. Lithos 120 (1–2), 74–95.

Gallastegui, J., Pulgar, J.A., Gallart, J., 2002. Initiation of an active margin at North Iberian continent–ocean transition. Tectonics 21. http://dx.doi.org/10.1029/2001TC901046.

Garate, J., Martin-Davila, J., Khazaradze, G., Echeverria, A., Asensio, E., Gil, A.J., de Lacy, M.C., Armenteros, J.A., Ruiz, A.M., Gallastegui, J., Alvarez-Lobato, F., Ayala, C., Rodriguez-Caderot, G., Galindo-Zaldivar, J., Rimi, A., Harnafi, M., 2014. Topo-Iberia project: CGPS crustal velocity field in the Iberian Peninsula and Morocco. GPS Solutions. http://dx.doi.org/10.1007/s10291-014-0387-3.

Gibbons, W., Moreno, T. (Eds.), 2002. The Geology of Spain. Geological Society, London (649 pp.).

Guimerà, J., Mas, R., Alonso, Á., 2004. Intraplate deformation in the NW Iberian Chain: Mesozoic extension and Tertiary contractional inversion. J. Geol. Soc. 161, 291–303.

Gutiérrez Alonso, G., Johnston, S.T., Weil, A.B., Pastor-Galán, D., Fernández-Suárez, J., 2012. Buckling an orogen: The Cantabrian Orocline. GSA Today 22 (7), 4–9. http://dx.doi.org/10.1130/GSATG141A.1.

Jiménez-Munt, I., Fernàndez, M., Vergés, J., Garcia-Castellanos, D., Fullea, J., Pérez-Gussinyé, M., Afonso, J.C., 2011. Decoupled crust-mantle accommodation of Africa-Eurasia convergence in the NW Moroccan margin. J. Geophys. Res. 116, B08403. http://dx.doi.org/10.1029/2010JB008105.

Jolivet, L., Faccenna, C., Piromallo, C., 2009. From mantle to crust: stretching the Mediterranean. Earth Planet. Sci. Lett. 285, 198–209. http://dx.doi.org/10.1016/j.epsl.2009.06.017.

Julivert, M., Fontboté, J. M., Ribeiro, A. and Conde, L., 1972. Mapa Tectónico de la Península Ibérica y Baleares, 1:1.000.000. Inst. Geol. Min. Esp. Madrid, 113 pp.

Kreemer, C., 2009. Absolute plate motions constrained by shear wave splitting orientations with implications for hot spot motions and mantle flow. J. Geophys. Res. 114, B10405. http://dx.doi.org/10.1029/2009JB006416.

Long, M.D., 2013. Constraints on subduction geodynamics from seismic anisotropy. Rev. Geophys. 51, 76–112. http://dx.doi.org/10.1002/rog.20008.

Long, M.D., Becker, Th.W., 2010. Mantle dynamics and seismic anisotropy. Earth Planet. Sci. Lett. 297 (2010), 341–354. http://dx.doi.org/10.1016/j.epsl.2010.06.036.

Martínez Catalán, J.R., Pérez-Estaún, A., Bastida, F., Pulgar, J.A., Marcos, A., 1990. West Asturian–Leonese Zone: structure. In: Dallmeyer, R.D., Martínez, E. (Eds.), Pre-Mesozoic Geology of Iberia. Springer-Verlag, Berlin, pp. 103–114.

Matte, Ph., 1991. Accretionary history and crustal evolution of the Variscan belt in Western Europe. Tectonophysics 196, 309–337.

Miller, M.S., Allam, A.A., Becker, Th.W., Di Leo, J.F., Wookey, J., 2013. Constraints on the tectonic evolution of the westernmost Mediterranean and northwestern Africa from shear wave splitting analysis. Earth Planet. Sci. Lett. 375, 234–235. http://dx.doi.org/10.1016/j.epsl.2013.05.036.

Missenard, Y., Cadoux, A., 2011. Can Moroccan Atlas lithospheric thinning and volcanism be induced by edge-driven convection? Terra Nova 00, 1–8. http://dx.doi.org/10.1111/j.1365-3121.2011.01033.x.

Morais, I., 2012. Structure of the Crust and Mantle Beneath Iberia and Western Mediterranean From P and S Receiver Functions and SKS Waveforms. (PhD Thesis). Univ. Lisboa.

Morais, I., Vinnik, L., Silveira, G., Kiselev, S., Matias, L., 2015. Mantle beneath the Gibraltar arc from receiver functions. Geophys. J. Int. 200, 1155–1171. http://dx.doi.org/10.1093/gji/ggu456.

Muñoz, J.A., 1992. Evolution of a continental collision belt: ECORS-Pyrenees crustal balanced cross-section. In: McClay, K.R. (Ed.), Thrust Tectonics. Chapman and Hall, London, pp. 235–246.
Negredo, A., Fernández, M., Torne, M., Doglioni, C., 1999. Numerical modeling of simultaneous extension and compression: the Valencia trough (western Mediterranean). Tectonics 18, 361–374.
Nicolas, A., Christensen, N.I., 1987. Formation of anisotropy in upper mantle peridotites. A review. In: Fuchs, K., Froidevaux, C. (Eds.), Composition, Structure and Dynamics of the Lithosphere–Asthenosphere System. AGU, Washington, pp. 137–154.
Pedreira, D., Pulgar, J.A., Gallart, J., Torne, M., 2007. Three-dimensional gravity and magnetic modeling of crustal indentation and wedging in the western Pyrenees–Cantabrian Mountains. J. Geophys. Res. 112. http://dx.doi.org/10.1029/2007JB005021.
Pedreira, D., Afonso, J.C., Pulgar, J.A., Gallastegui, J., Carballo, A., Fernàndez, M., García-Castellanos, D., Jiménez-Munt, I., Semprich, J., Garcia-Morena, O., 2015. Geophysical–petrological modeling of the lithosphere beneath the Cantabrian Mountains and North-Iberian margin: geodynamic implications. Lithos (accepted for publication).
Pérez-Estaún, A., Bastida, F., Alonso, J.L., Marquínez, J., Aller, J., Álvarez-Marrón, J., Marcos, A., Pulgar, J.A., 1988. A thin-skinned tectonics model for an arcuate fold and thrust belt: the Cantabrian Zone (Variscan Ibero-Armorican Arc). Tectonics 7, 517–537.
Pérez-Estaún, A., Pulgar, J.A., Banda, E., Álvarez-Marrón, J., ESCIN Research Group, 1994. Crustal structure of the external variscides in northwest Spain from deep seismic reflection profiling. Tectonophysics 232, 91–118.
Ranero, C.R., Pérez-Gussinyé, M., 2010. Sequential faulting explains the asymmetry and extension discrepancy of conjugate margins. Nature. http://dx.doi.org/10.1038/nature09520.
Savage, M.K., 1999. Seismic anisotropy and mantle deformation: what have we learned from shear wave splitting? Rev. Geophys. 37, 65–106.
Sibuet, J-Cl, Srivastava, S.P., Spakman, W., 2004. Pyrenean orogeny and plate kinematics. J. Geophys. Res. 109, B08104. http://dx.doi.org/10.1029/2003JB002514.
Silver, P.G., 1996. Seismic anisotropy beneath the continents: probing the depths of geology. Ann. Rev. Earth Planet. Sci. 24, 385–432.
Silver, P.G., Chan, W.W., 1988. Implications for continental structure and evolution from seismic anisotropy. Nature 355, 34–39.
Silver, P.G., Savage, M.K., 1994. The interpretation of shear-wave splitting parameters in the presence of two anisotropic layers. Geophys. J. Int. 119, 949–963.
Sutra, E., Manatschal, G., Mohn, G., Unternehr, P., 2013. Quantification and restoration of extensional deformation along the Western Iberia and Newfoundland rifted margins. Geochem. Geophys. Geosyst. 14, 2575–2597. http://dx.doi.org/10.1002/ggge.20135.
Tian, X., Zhang, J., Si, S., Wang, J., Chen, Y., Zhang, Z., 2011. SKS splitting measurements with horizontal component misalignment. Geophys. J. Int. 185 (1), 329–340. http://dx.doi.org/10.1111/j.1365-246X.2011.04936.x.
Tucholke, B.E., Sawyer, D.S., Sibuet, J.C., 2007. Breakup of the Newfoundland Iberia rift. Geol. Soc. Lond., Spec. Publ. 282, 9–46. http://dx.doi.org/10.1144/SP282.2.
Vauchez, A., Tommasi, A., Mainprice, D., 2012. Faults (shear zones) in the Earth's mantle. Tectonophysics 558, 1–27. http://dx.doi.org/10.1016/j.tecto.2012.06.006.
Vinnik, L., Farra, V., Romanowicz, B., 1989. Azimuthal anisotropy in the Earth from observations of SKS at GEOSCOPE and NARS broadband stations. Bull. Seismol. Soc. Am. 79, 1542–1555.
Vinnik, L.P., Makeyeva, L.I., Milev, A., Usenko, A.Yu., 1992. Global patterns of azimuthal anisotropy and deformations in the continental mantle. Geophys. J. Int. 111, 433–447.
Vinnik, L., Kiselev, S., Weber, M., Oreshin, S., Makeyeva, L., 2012. Frozen and active seismic anisotropy beneath southern Africa. Geophys. Res. Lett. 39, 1–6.
Wessel, P., Smith, W.H.F., 1998. New, improved version of the generic mapping tool released. EOS Trans. Am. Geophys. Union 47, 576.
Wüstefeld, A., Bokelmann, G., Zaroli, Ch., Barruol, G., 2008. SplitLab: a shear-wave splitting environment in Matlab. Comput. Geosci. 34, 515–528. http://dx.doi.org/10.1016/j.cageo.2007.08.002.
Wüstefeld, A., Bokelmann, G.H.R., Barruol, G., Montagner, J.-P., 2009. Identifying global seismic anisotropy patterns by correlating shear-wave splitting and surface waves data. Phys. Earth Planet. Inter. 176 (3–4), 198–212. http://dx.doi.org/10.1016/j.pepi.2009.05.006 (database available online at http://www.gm.univ-montp2.fr/splitting/DB/).
Yuan, K., Beghein, C., 2013. Seismic anisotropy changes across upper mantle phase transitions. Earth Planet. Sci. Lett. 374, 132–144. http://dx.doi.org/10.1016/j.epsl.2013.05.031.
Zandt, G., Humphreys, E., 2008. Toroidal mantle flow through the western US slab window. Geology 36, 295–298.